



Published in final edited form as:

Hear Res. 2016 May ; 335: 94–104. doi:10.1016/j.heares.2016.02.006.

Perinatal Thiamine Deficiency Causes Cochlear Innervation Abnormalities in Mice

Stéphane F. Maison^{1,2,3}, Yanbo Yin^{1,2}, Leslie D. Liberman², and M. Charles Liberman^{1,2,3}

¹Department of Otology and Laryngology, Harvard Medical School, Boston MA

²Eaton-Peabody Laboratory, Massachusetts Eye & Ear Infirmary, Boston MA

³Harvard Program in Speech and Hearing Bioscience and Technology, Boston MA

Abstract

Neonatal thiamine deficiency can cause auditory neuropathy in humans. To probe the underlying cochlear pathology, mice were maintained on a thiamine-free or low-thiamine diet during fetal development or early postnatal life. At postnatal ages from 18 days to 22 wks, cochlear function was tested and cochlear histopathology analyzed by plastic sections and cochlear epithelial whole-mounts immunostained for neuronal and synaptic markers. Although none of the thiamine-deprivation protocols resulted in any loss of hair cells or any obvious abnormalities in the non-sensory structures of the cochlear duct, all the experimental groups showed significant anomalies in the afferent or efferent innervation. Afferent synaptic counts in the inner and outer hair cell areas were reduced, as was the efferent innervation density in both the outer and inner hair cell areas. As expected for primary neural degeneration, the thresholds for distortion product otoacoustic emissions were not affected, and as expected for subtotal hair cell de-afferentation, the suprathreshold amplitudes of auditory brainstem responses were more affected than the response thresholds. We conclude that the auditory neuropathy from thiamine deprivation could be produced by loss of inner hair cell synapses.

Keywords

Thiamine; Development; Auditory neuropathy; Olivocochlear

Introduction

Auditory neuropathy is a type of sensorineural hearing loss resulting from disorders affecting inner hair cells (IHCs), cochlear sensory neurons or the synapses between them (for review, see Starr and Rance, 2015). It can be congenital (Bahmad et al., 2007; Santarelli et al., 2009; Pangrsic et al., 2010) or acquired (Beutner et al., 2007), and it is diagnosed

Correspondence to: Stéphane F. Maison, Ph.D., Eaton-Peabody Laboratory, Massachusetts Eye and Ear Infirmary, 243 Charles St., Boston, MA 02114-3096, USA. Tel: 617-573-3745, Fax: 617-720-4408, stephane_maison@meei.harvard.edu.

Publisher's Disclaimer: This is a PDF file of an unedited manuscript that has been accepted for publication. As a service to our customers we are providing this early version of the manuscript. The manuscript will undergo copyediting, typesetting, and review of the resulting proof before it is published in its final citable form. Please note that during the production process errors may be discovered which could affect the content, and all legal disclaimers that apply to the journal pertain.

based on the presence of otoacoustic emissions despite an absent or highly disorganized auditory brainstem response (Hood, 2015). A number of risk factors have been identified. For example a high incidence of auditory neuropathy is found in infants born prematurely (Xoinis et al., 2007). Recently, a study of infant temporal bones revealed that 30% of preterm babies who died in the NICU had selective inner hair cell (IHC) loss, while only 3% of full-term infants presented such a phenotype (Amatuzzi et al., 2011). This high prevalence for such a rare histopathology (Schuknecht, 1993) suggested that selective IHC loss might be a common cause of auditory neuropathy.

Our group recently reported a link between IHC loss and thiamine, a water-soluble vitamin (B1) required for intermediary metabolism. Patients with the syndromic disorder known as Thiamine-Responsive Megaloblastic Anemia (TRMA) have hearing loss in addition to the pathognomonic anemic symptoms (Fleming et al., 1999, 2001). Genetic analysis revealed a mutation in one of the two transporters involved in trafficking thiamine across cell membranes: *SLC19A2*. Targeted deletion of *SLC19A2* in mice causes auditory neuropathy and selective IHC loss when animals are challenged with a diet low in thiamine (Lieberman et al., 2006).

Further evidence for a link between thiamine and auditory neuropathy was provided by a study of children who were bottle-fed from birth with an infant formula completely lacking in thiamine due to a manufacturing error. As infants, these children were hospitalized with a variety of neurological symptoms consistent with thiamine deficiency, collectively known as Wernicke's encephalopathy (Fattal-Valevski et al., 2005). Continued follow-up showed an extraordinarily high percentage of auditory neuropathy (Attias et al., 2012).

Combining all these observations, we wondered if the link between prematurity and auditory neuropathy might reflect an immaturity of thiamine transporters in preterm infants coupled with varying standards for thiamine supplementation during NICU stays (Friel et al., 2001). To gain insight into the effects of thiamine deprivation in the perinatal period, we deprived mice of dietary thiamine during pregnancy and/or nursing. We let the offspring mature to varying ages, measured cochlear function by ABRs and DPOAEs and evaluated the degeneration of hair cells and their afferent and efferent innervation. We found no evidence for selective IHC loss; however, many thiamine-deprived animals showed dramatic abnormalities in the cochlear afferent and efferent innervation, and associated cochlear functional abnormalities consistent with the diagnosis of auditory neuropathy.

Materials and Methods

Animals, Procedure and Statistical Analysis

CBA/CaJ mice were used in all experiments. To control thiamine intake, a thiamine-free chow was obtained from TestDiet® (TestDiet.com) in powdered form. The formulation was identical, in all other respects, to that established for use in mice by the American Institute of Nutrition. The desired thiamine concentration was adjusted by addition of powdered thiamine diluted in water. The mixture was provided as a moist gruel.

Mice were assigned to one of three groups: 1) *Control* animals, which were fed with regular chow (22 mg/kg thiamine); 2) *Low-Thiamine* animals, in which thiamine-free chow was supplemented with 0.2 mg/kg of thiamine and 3) *No Thiamine* animals, which received a thiamine-free chow. For the last two groups, thiamine deprivation was either implemented prenatally (*Pre*) or postnatally (*Post*) for durations ranging from 2 to 6 weeks (Fig. 1).

Cochlear function was assessed bilaterally in each mouse reaching at least 6 wks of age via auditory brainstem responses (ABRs) and distortion product otoacoustic emissions (DPOAEs). After the final cochlear function test, cochleas were fixed by intracardiac perfusion and removed for histological processing and light-microscopic analysis of cochlear degeneration. All procedures were approved by the IACUC of the Massachusetts Eye and Ear Infirmary. Two-way repeated-measure ANOVAs, adjusted with the Holm-Bonferroni correction, were used to assess the statistical significance of group differences.

Cochlear Function Tests

For measuring ABRs and DPOAEs, animals were anesthetized with xylazine (20 mg/kg, i.p.) and ketamine (100 mg/kg, i.p.) and placed in an acoustically and electrically shielded room maintained at 32°C. Acoustic stimuli were delivered through a custom acoustic system consisting of two miniature dynamic earphones used as sound sources (CUI CDMG15008-03A) and an electret condenser microphone (Knowles FG-23329-PO7) coupled to a probe tube to measure sound pressure near the eardrum.

Digital stimulus generation and response processing were handled by digital I-O boards from National Instruments driven by custom LabVIEW software. For ABRs, stimuli were 5-msec tone pips (0.5 msec \cos^2 rise-fall) delivered in alternating polarity at 35/sec. Electrical responses were sampled via Grass needle electrodes at the vertex and pinna with a ground reference near the tail and amplified 10,000 \times with a 0.3 - 3 kHz passband. Responses to as many as 1024 stimuli were averaged at each sound pressure level, as level was varied in 5 dB steps from below threshold up to 80 dB SPL. For DPOAEs, stimuli were two primary tones f_1 and f_2 ($f_2/f_1 = 1.2$), with f_1 level always 10 dB above f_2 level. Primaries were swept in 5 dB steps from 20 to 80 dB SPL (for f_2). The DPOAE at $2f_1-f_2$ was extracted from the ear canal sound pressure after both waveform and spectral averaging. Noise floor was defined as the average of 6 spectral points below, and 6 above, the $2f_1-f_2$ point. Threshold was computed, by interpolation, as the primary level (f_2) required to produce a DPOAE of 0 dB SPL.

Cochlear Processing, Immunostaining and Histological Analysis

Mice were perfused intracardially with 4% paraformaldehyde in phosphate buffer. Cochleas were processed in one of two ways. For evaluation of all structures of the cochlear duct, ears were post-fixed in osmium tetroxide (1%) and then decalcified, plastic-embedded and serially sectioned at 40 microns (Wang et al., 2002). For hair cell counts and innervation analysis, cochleas were decalcified, dissected into half-turns and permeabilized by freeze/thawing. The half-turns were blocked in 5% normal horse serum (NHS) with 0.3% Triton X-100 (TX) in PBS for 1 hr, followed by incubation for \sim 19 hrs at 37°C in primary antibodies diluted in 1% NHS with 0.3% TritonX. Primary antibodies included 1) mouse

(IgG1) anti-CtBP2 (BD Biosciences #612044) at 1:200 to visualize presynaptic ribbons, 2) mouse (IgG2a) anti-GluA2 (Millipore #MAB397) at 1:2000 to visualize postsynaptic glutamate receptor patches, and 3) rabbit anti-VAT (Vesicular Acetylcholine Transporter; Abcam #ab68986) at 1:200 to allow quantification cochlear efferent terminals. The vast majority of efferent fibers are cholinergic and therefore VAT-positive. We did not immunostain the small dopaminergic population (Darrow et al., 2006) because it is very sparse, and therefore difficult to assess. Primary incubations were followed by two sequential 60-min incubations at 37°C in species-appropriate secondary antibodies with 0.3% TritonX.

Histological analysis of cochlear epithelial wholemounts was based on high-power confocal z-stacks of the sensory epithelium obtained at half-octave intervals along the cochlea from 5.6 to 64 kHz. To identify regions of interest, cochlear lengths were obtained for each case by tracing low-power images of the dissected pieces using a custom ImageJ plug-in that translates cochlear position into frequency using the mouse frequency map (Taberner and Liberman, 2005). Confocal z-stacks were obtained with a glycerol-immersion objective (63×, numerical aperture = 1.3) at 3.17× digital zoom on a Leica TCS SP5. Image spacing in the z plane was 0.25 μm, and the z-span was adjusted for each stack to include all synaptic elements in all of the 9-12 hair cells from each row included in each stack, typically requiring ~100 images per stack. Two adjacent stacks were always obtained in each cochlear region sampled.

Presynaptic ribbons and/or postsynaptic glutamate receptor patches were counted from each confocal z-stack using the *connected components* tool in Amira® (Visage Imaging), which finds and displays each voxel space in an image stack containing pixel values greater than a user-set criterion. To quantitatively assess the pairing of pre- and post-synaptic elements, we used custom software that extracts the voxel space within 1 μm around each ribbon (or receptor patch) and produces a thumbnail array of these miniature projections, that can be scanned to count synapses (i.e. ribbons with closely apposed receptor patches) vs. orphan ribbons or orphan receptor patches (Liberman et al., 2011).

Hair cells in each z-stack were counted by increasing the image output-gain (gamma adjust): Inner hair cell nuclei stain faintly with the CtBP2 antibody, and the outer hair cell somata are visible via their faint background label in several confocal channels, as well as by the presence of synaptic ribbons, even when the efferent terminals are missing. The synaptic count in each z-stack was divided by the number of hair cells.

The degree of de-efferentation was assessed in both inner and outer hair cell areas from maximum projections of the VAT-immunostaining in the z-stacks. In both inner and outer hair cell area, the OC innervation was quantified by applying the auto-thresholding algorithm from ImageJ and counting the total number of pixels in maximum projections.

Results

Normal mouse chow contains 22 mg/kg thiamine. In this study, mice were fed with a chow containing either 1) 22 mg/kg thiamine, 2) 0.2 mg/kg thiamine or 3) 0 mg/kg thiamine. As

schematized in Figure 1, thiamine deprivation was implemented either prenatally or postnatally for durations ranging from 2 to 6 wks. There were no pregnancies when mice were fed 0 mg/kg thiamine for more than 3 wks. Under a low-thiamine diet (0.2 mg/kg), pregnancies went to term only when thiamine restriction lasted less than 3 wks (*Pre-3*, *Pre-2a*, *Pre-2b*). Postnatal removal of all thiamine led to progressive weakening if extended beyond 2 wks; thus one group was terminated at 18 days (*Post-2.5*). When postnatal thiamine absence was limited to 2 wks (*Post-2*) or when a low-thiamine diet was imposed postnatally for 3 wks (*Post-3*), pups were able to mature, with no obvious physical or behavioral abnormalities, and without any increased mortality over their littermates raised with normal dietary thiamine. Thus, apart from the *Post-2.5* group there is no over evidence of general neurological problems.

As schematized in Figure 1, animals from different groups were allowed to mature until 18 days (*Post-2.5*), 6 wks (*Pre-3*, *Pre-2a* and *Pre-2b*) or 22 wks (*Post-2*) before final cochlear function test and/or cochlear tissue harvest. None of the groups showed any significant loss of inner or outer hair cells (Fig. 2), compared to controls, as assessed by two-way ANOVA, even in the animals that were sacrificed at P18 because they were extremely weakened by the complete lack of postnatal thiamine (*Post-2.5* group in Fig. 2). Despite the lack of hair cell degeneration, there were significant anomalies in the afferent and efferent innervation. Within each group, there was also significant heterogeneity in the severity of the dysmorphology. Six ears from the *Post-2.5* group were evaluated by serially sectioned, plastic embedded sections: despite the innervation anomalies described below, there were no obvious abnormalities in any cochlear structures outside the sensory epithelium, including the stria vascularis, the spiral ligament, the limbus or the spiral ganglion (Fig. 3)

Postnatal thiamine deprivation

Overall, the most severely affected groups were the animals that were totally deprived of dietary thiamine immediately after birth. By P18 (*Post-2.5* group), such animals were showing signs of physical distress, thus the cochleas were fixed and harvested without attempting functional measurements. In a normal mouse at P18, the afferent innervation of the IHC is almost completely developed (Fig. 4A): the subnuclear regions of the IHCs are studded with synaptic puncta. Here, we immunostained pre-synaptic ribbons with antibodies to CtBP2 (Schmitz et al., 2000; Khimich et al., 2005) and post-synaptic receptor plaques with antibodies to an AMPA-type glutamate receptor, GluA2 (Matsubara et al., 1996). The region underneath the IHCs is also heavily innervated by cholinergic terminals of the lateral olivocochlear (LOC) system, which we immunostained with antibodies to VAT (vesicular acetylcholine transporter). These VAT-positive puncta indicate sites of synaptic contact between LOC terminals and the peripheral dendrites of cochlear nerve fibers (Maison et al., 2003).

As shown in Figure 4B, ears with 18 days of complete postnatal thiamine deprivation (*Post-2.5*) show dramatic loss of pre-synaptic ribbons and an even more dramatic loss of synaptic complexes, due to the absence of GluA2-positive puncta opposite many CtBP2-positive presynaptic ribbons. Many CtBP2-positive puncta are found near the cuticular plates of the IHCs (red arrow in Fig. 4B right), where they are never seen in normal ears at this age.

There appears to be an overall decrease in the density of LOC innervation. The prominent background staining in the green channel was seen in all ears from this group and never in controls, though both types were routinely stained in the same batches.

Quantification of cochlear afferent and efferent innervation in these *Post-2.5* ears shows that not a single pup had a normal innervation pattern (Fig. 5). Some ears were more severely affected than others, and affected ears tended to show dysmorphology in both afferent and efferent innervation. Even the most affected case (334), which had virtually no IHC synapses (Fig. 5B), showed no obvious abnormalities in spiral ganglion from the opposite ear (Fig. 3). The reduction in IHC synaptic numbers *re* control (Fig. 5B) was highly significant across all cases (two-way ANOVA: $F=30.4$, $p<0.001$), with the decrement in individual cases ranging from $\sim 25\%$ to $\sim 100\%$. LOC efferent density (Fig. 5A) was significantly altered under thiamine deprivation when compared to age-matched controls (two-way ANOVA: $df=1$, $F=7.1$, $p=0.026$) with respectively increased and decreased efferent innervation from the apex to the base of the cochlea. In the OHC area, the reduction of medial olivocochlear (MOC) terminal density (Fig. 5C) was significant across all cases (two-way ANOVA: $df=1$, $F=6.8$, $p=0.029$), but especially striking in the same three cases with reduced IHC synaptic counts. Lastly, as shown in Figure 5D, OHC ribbon counts were reduced in the apex, especially in one case, but the differences failed to reach significance when compared, as a group, to age-matched controls (two-way ANOVA (5-11 kHz): $df=1$, $F=4.1$, $p=0.081$).

Mice on a thiamine-free diet for 2 wks postnatally (*Post-2*) also showed progressive weakening, but recovered once normal dietary thiamine was introduced. These animals were allowed to mature to 22 wks before final cochlear function test and cochlear tissue harvest. As shown in Figure 6, ears in this group also showed significant abnormalities in cochlear innervation, particularly a decrease in the number of IHC synapses (Fig. 6Dxy), an increase in the number of orphan ribbons (Fig. 6Dzy) in the IHC regions (as noted above), and a dramatic decrease in the density of MOC efferent terminals in OHC area (Fig. 6C).

As shown more quantitatively in Figure 7, the severity of the innervation anomalies differed greatly within the group, but two of the ears (red symbols) showed dramatic changes in all four cochlear neuronal types. Overall, the abnormalities were greater in the apical half of the cochlea. LOC efferent density (Fig. 7A) was significantly reduced along the entire cochlear spiral (two-way ANOVA: $df=1$, $F=44.0$, $p<0.001$) with losses $> 50\%$ in apical regions. MOC density (Fig. 7C) was significantly reduced (two-way ANOVA: $df=1$, $F=7.2$, $p=0.02$), though the differences are dominated by apical measures in two cochleas. The loss of OHC ribbon synapses was highly significant (Fig. 7D, two-way ANOVA: $df=1$, $F=25.2$, $p<0.001$), but the differences were clearly greatest in apical regions. IHC synapses were severely affected in the apical half of two cases, yet close to normal in five others (Fig. 7B). As a group, the synaptic-count differences from Control were not statistically significant (two-way ANOVA, $df=1$, $F=4.7$, $p=0.052$).

In the *Post-2* group, cochlear responses were assessed at 22 wks. As a group, cochlear thresholds were normal *re* age-matched controls, as measured by ABRs (Fig. 8A, two-way ANOVA, $df=1$, $F=1.0$, $p=0.503$) or DPOAEs (Fig. 8B, two-way ANOVA, $df=1$, $F=2.3$,

$p=0.368$). As a group, DPOAE suprathreshold amplitudes were also normal (Fig. 8D,F, two-way ANOVA: 8kHz – $df=1$, $F=3.0$, $p=0.094$; 32kHz – $df=1$, $F=2.3$, $p>0.05$). On an individual ear basis, two ears showed slightly higher DPOAE thresholds at high frequencies accompanied by markedly lower DPOAE suprathreshold amplitudes (green symbols in Fig. 8B,F). Although these ears showed reduced OHC synaptic ribbon counts (Fig. 7D, the innervation abnormalities were no greater in these two cases than in the other *Post-2* ears.

Supra-threshold neural responses (ABR Wave 1) were significantly depressed at both high and low frequencies (Fig. 8C,E, two-way ANOVA: 8kHz – $df=1$, $F=22.5$, $p<0.001$; 32kHz – $df=1$, $F=13.1$, $p=0.002$). Amplitude decrements were more striking at low frequencies than high frequencies. Note that the two cases with dramatic loss IHC synapses in apical regions (Fig. 7B) are also the two cases with dramatically reduced Wave 1 amplitudes at 8 kHz (Fig. 8C). The reasons for the reductions in Wave 1 amplitudes at high frequencies (Fig. 8E) are less clear, although two of the cases also show reduced DPOAE amplitudes (Fig. 8F) suggestive of OHC dysfunction.

Prenatal thiamine deprivation

Cochlear innervation anomalies in *Pre-3* animals (born to mothers on a low-thiamine diet for 3 wks prior to giving birth) were generally similar to those in postnatally deprived animals, though not as striking. As a group, the *Pre-3* ears were significantly different, by two-way ANOVA, from age-matched controls on all four measures of afferent and efferent innervation density: LOC (Fig. 9A) $df=1$, $F=5.6$, $p=0.034$; IHC (Fig. 9B) $df=1$, $F=6.0$, $p=0.029$; MOC (Fig. 9C) $df=1$, $F=10.5$, $p=0.006$; and OHC (Fig. 9D) $df=1$, $F=6.0$, $p=0.044$.

The most striking differences were seen in the MOC innervation density Fig. 9C, where the decrements were largest near the cochlear base. Loss of IHC synapses (Fig. 9B) and OHC ribbons (Fig. 9D) were seen throughout the cochlear spiral, but losses were largest near the apex. Cochlear function was measured in all the *Pre-3* animals, by both ABRs and DPOAEs, however all threshold and suprathreshold measures were statistically indistinguishable from those obtained in age-matched controls (Fig. 9E,F).

When the pre-natal thiamine restriction was only 2 wks in duration (*Pre-2* in Figure 1), the innervation abnormalities were confined to the efferent innervation (Fig. 10). The LOC density was slightly reduced in all cochlear regions (two-way ANOVA, $df=1$, $F=12.4$, $p=0.004$) and the MOC innervation was slightly reduced ($df=1$, $F=10.1$ $p=0.008$). The differences in both cases were statistically significant and were seen mainly in the apical half of the cochlea. Synaptic counts in both IHC and OHC areas were statistically indistinguishable from controls (two-way ANOVA, $df=1$, $F=3.4$ $p=0.089$ and $df=1$, $F=0.2$ $p=0.641$, respectively). As with the 3-wk thiamine restriction, cochlear function was measured in all animals in this group, but threshold and suprathreshold measures were statistically indistinguishable from those obtained in age-matched controls (data not shown).

Discussion

A. Cochlear synaptopathy and cochlear development

Here, we investigated the effects of thiamine deficiency on the mouse cochlea during embryonic and postnatal development. We were inspired by a clinical report describing a high rate of auditory neuropathy in newborns fed with a commercial infant formula totally lacking in thiamine (Fattal-Valevski et al., 2005; Attias et al., 2012), also known vitamin B1, a key co-factor in intermediary metabolism. The diagnosis of auditory neuropathy in humans is based on the presence of otoacoustic emissions despite the lack of a clear ABR (Hood, 2015). The presence of otoacoustic emissions indicates that the cochlear sensory epithelium, the stria vascularis and specifically the outer hair cells must be basically intact. The absence of the ABR, including wave 1, could result from a loss of inner hair cells, cochlear afferent synapses and/or the cochlear sensory neurons *per se*. The present results suggest that the neuropathy in this clinical report may have arisen from loss of cochlear nerve synapses in the IHC area.

Maternal thiamine deprivation will lead to thiamine-deprived offspring (Bamji, 1976). Here, we compared the effects of prenatal deprivation of 2-3 wks duration and postnatal deprivation of 2-3 wks duration. The cochlear effects of postnatal deprivation were more clearcut, however, complete prenatal deprivation could not be studied, because no offspring were produced. The gestation period in mice is 19 days, and the first two postnatal weeks are a period of active cochlear synaptogenesis. At P0, the production of hair cells and cochlear neurons is complete, and the peripheral processes of cochlear nerve fibers and olivocochlear efferent neurons have reached the sensory epithelium (Barald and Kelley, 2004). However, the normal innervation patterns are not established until at least P10. At P0, each IHC contains 40-50 presynaptic ribbons, scattered throughout the cytoplasm (Huang et al. 2012), where they are unpaired with postsynaptic elements. By P12, the number of ribbons falls to 10-20 per IHC (Huang et al., 2012), as seen in the adult control group (Fig. 2B), and they are found exclusively at the IHC basolateral membrane, where most are paired with an AMPA-receptor patch on a cochlear-nerve terminal. At P0, there are only scattered efferent (VAT-positive) terminals in the OHC area; by P18, the olivocochlear innervation density looks adult-like (Maison, Adams and Liberman, 2002).

Present results show that thiamine restriction during this time of active IHC synaptogenesis has dramatic consequences for the development of the cochlear innervation. None of the thiamine-deprived groups showed any significant loss of hair cells (Fig. 2), or any obvious pathology in any of the accessory structures of the cochlear duct such as the stria vascularis, spiral ligament, spiral limbus, etc (Fig. 3). Thus, in the cochlea it is the neural structures that appear to be the most vulnerable to thiamine deficiency. In the experimental group with all dietary thiamine removed from mothers at P0, ears examined at P18 (*Post-2.5* group) had IHC synaptic counts that were < 50% of normal in 5 out of 6 cases including 2 cases where no postsynaptic densities could be found (Fig. 5B). There were numerous orphan ribbons, and the normal modiolar-pillar gradient of ribbon morphology (Yin et al., 2014) failed to develop (Fig. 7). Experimental groups with a milder thiamine restriction pre- or post-natally also showed IHC synaptopathy, but to a lesser degree.

Given that many aspects of cochlear innervation are adult-like at P12 (Huang et al. 2012), it is unlikely that cochlear neuropathies induced by thiamine deprivation during the first two weeks of life would be reversible by thiamine supplementation at times beyond this developmental window. Although there is spontaneous regeneration of spiral ganglion cell peripheral dendrites and of their synaptic connections with inner hair cells in the neonatal (P6) rat ear after drug-induced synaptopathy (Wang and Green, 2011), there is no evidence for any regeneration of cochlear nerve peripheral synapses in the adult mouse after noise-induced synaptopathy (Kujawa and Liberman, 2009). On the other hand, noise-induced synaptopathy can be partially rescued by overexpression of neurotrophin-3 (Wan and Corfas, 2015), a molecular signal of particular importance to cochlear neuronal survival in the adult. It is possible that thiamine-induced synaptopathy could also be rescued in similar fashion, given that, as with noise-induced and age-related synaptopathies (Kujawa and Liberman, 2009; Sergeyenko et al., 2013), the loss of spiral ganglion cells seems significantly delayed with respect to the loss of synapses (Fig. 3).

B. Cochlear synaptopathy and the olivocochlear efferents

In humans, adult-onset thiamine deficiency, known as Wernicke's encephalopathy, is seen in alcoholics as well as patients with impaired nutrition from gastrointestinal disease (Kril, 1996). The pathology is characterized by diffuse neurological symptoms including mental confusion, abnormal eye movements, and unsteady gait. Histologically, neuronal loss, gliosis and vascular damage is seen, particularly in regions surrounding the third and fourth ventricles and the cerebral aqueduct, including the thalamus, hypothalamus, mammillary nucleus and the floor of the fourth ventricle (Victor et al., 1989; Harata and Iwasaki, 1996; Elefante et al., 2012; Zhong et al., 2005). Affected areas are often adjacent to intact regions, with sharp demarcation of the pathologic changes (Harata and Iwasaki, 1996). MRI-based studies also identify the paraventricular regions of the fourth ventricle as particularly vulnerable areas in cases of thiamine deficiency (Drayer, 1988; Donnal et al., 1990; Gallucci et al., 1990).

In animal studies, the brainstem regions consistently damaged under thiamine deficiency are the inferior and superior colliculi, lateral and superior vestibular nuclei, and the inferior olives (Langlais et al. 1996). Damage to the superior olivary complex and locus coeruleus nuclei were noted when thiamine deprivation was more severe (Zhang et al., 1994), with neuronal loss thought to result from an excitotoxic mechanism mediated by glutamatergic NMDA receptors (Zhang et al., 1995; Zhong et al., 2005). Here, we show that both MOC and LOC efferent systems, two neuronal feedback pathways arising from the superior olivary complex, are susceptible to thiamine deprivation. Indeed, as we decreased the degree and duration of the thiamine deficiency, the most vulnerable structures in the cochlea appeared to be the LOC and MOC innervation (Fig. 10). In the adult ear, prior studies from our group have shown that 1) surgical lesions to the LOC and MOC systems can lead to synaptopathy in the IHC area (Maison et al., 2013; Liberman et al., 2014) and that chronic sound deprivation by removal of the eardrum can also lead to dramatic loss of LOC innervation density as well as IHC synaptopathy (Liberman et al., 2015).

Thus it is possible, in thiamine deficiency in the neonate, that the first affected elements are the cochlear efferents, and that the loss of the OC system, and particularly the loss of the LOC innervation, ultimately leads to loss of cochlear afferent synapses. Indeed, the increased synaptopathy among apical IHCs seen in some of the thiamine-deprived groups (Fig. 7B, 9B) is similar to that seen after surgical de-efferentation (See Fig. 6B in Liberman et al. 2014), as well as in the aging ear (see Fig. 5 in Sergeyenko et al., 2013). However, the reasons for this differential vulnerability are unclear. The trend runs counter to the general rule that the cochlear base is more vulnerable than the apex and does not obviously follow from the observation that both LOC and MOC innervation density is normally highest in the middle of the cochlear spiral (Maison et al., 2003). Indeed, in noise-induced synaptopathy following mid-frequency exposure, the apex is spared and the damage spreads asymmetrically towards the base (Kujawa and Liberman, 2009) as might have been predicted from the patterns of noise-induced hair cell loss and threshold shift (Wang et al., 2002).

It is possible that the increased prevalence of auditory neuropathy in premature infants has to do with immaturity in the thiamine absorption system in the neonatal ear. Regardless of the precise parallels between these animal experiments and the human diagnosis of auditory neuropathy, the present results add to the growing evidence that inner hair cell synapses are among the most vulnerable elements in the inner ear and that inner hair cell synaptopathy is a major contributor to the perceptual impairments in sensorineural hearing losses of many etiologies (Kujawa and Liberman, 2015).

Acknowledgments

Research supported by grants from the NIDCD: R21 DC 012599 and P30 DC 05209.

References Cited

- Amatuzzi M, Liberman MC, Northrop C. Selective inner hair cell loss in prematurity: a temporal bone study of infants from a neonatal intensive care unit. *J Assoc Res Otolaryngol.* 2011; 12:595–604. [PubMed: 21674215]
- Attias J, Raveh E, Aizer-Dannon A, Bloch-Mimouni A, Fattal-Valevski A. Auditory system dysfunction due to infantile thiamine deficiency: long-term auditory sequelae. *Audiol Neurootol.* 2012; 17:309–320. [PubMed: 22739497]
- Bahmad F Jr, Merchant SN, Nadol JB Jr, Tranebjaerg L. Otopathology in Mohr-Tranebjaerg syndrome. *Laryngoscope.* 2007; 117:1202–1208. [PubMed: 17471106]
- Bamji MS. Enzymic evaluation of thiamin, riboflavin and pyridoxine status of parturient women and their newborn infants. *Br J Nutr.* 1976; 35:259–265. [PubMed: 1252400]
- Barald KF, Kelley MW. From placode to polarization: new tunes in inner ear development. *Development.* 2004; 131:4119–4130. [PubMed: 15319325]
- Beutner D, Foerst A, Lang-Roth R, von Wedel H, Walger M. Risk factors for auditory neuropathy/auditory synaptopathy. *ORL J Otorhinolaryngol Relat Spec.* 2007; 69:239–244. [PubMed: 17409783]
- Darrow KN, Simons EJ, Dodds L, Liberman MC. Dopaminergic innervation of the mouse inner ear: evidence for a separate cytochemical group of cochlear efferent fibers. *J Comp Neurol.* 2006; 498:403–414. [PubMed: 16871528]
- Donnal JF, Heinz ER, Burger PC. MR of reversible thalamic lesions in Wernicke syndrome. *AJNR Am J Neuroradiol.* 1990; 11:893–894. [PubMed: 2120992]

- Drayer BP. Imaging of the aging brain. Part II. Pathologic conditions. *Radiology*. 1988; 166:797–806. [PubMed: 3277248]
- Elefante A, Puoti G, Senese R, Coppola C, Russo C, Tortora F, de Dvitiis O, Brunetti A. Non-alcoholic acute Wernicke's encephalopathy: role of MRI in non typical cases. *Eur J Radiol*. 2012; 81:4099–4104. [PubMed: 22954409]
- Fattal-Valevski A, Kesler A, Sela BA, Nitzan-Kaluski D, Rotstein M, Mesterman R, Toledano-Alhadeef H, Stolovitch C, Hoffmann C, Globus O, Eshel G. Outbreak of life-threatening thiamine deficiency in infants in Israel caused by a defective soy-based formula. *Pediatrics*. 2005; 115:233–238. [PubMed: 15866857]
- Fleming JC, Tartaglino E, Steinkamp MP, Schorderet DF, Cohen N, Neufeld EJ. The gene mutated in thiamine-responsive anaemia with diabetes and deafness (TRMA) encodes a functional thiamine transporter. *Nat Genet*. 1999; 22:305–308. [PubMed: 10391222]
- Fleming JC, Steinkamp MP, Kawatsuji R, Tartaglino E, Pinkus JL, Pinkus GS, Fleming MD, Neufeld EJ. Characterization of a murine high-affinity thiamine transporter, Slc19a2. *Mol Genet Metab*. 2001; 74:273–280. [PubMed: 11592824]
- Friel JK, Bessie JC, Belkhole SL, Edgecombe C, Steele-Rodway M, Downton G, Kwa PG, Aziz K. Thiamine, riboflavin, pyridoxine, and vitamin C status in premature infants receiving parenteral and enteral nutrition. *J Pediatr Gastroenterol Nutr*. 2001; 33:64–69. [PubMed: 11479410]
- Gallucci M, Bozzao A, Splendiani A, Masciocchi C, Passariello R. Wernicke encephalopathy: MR findings in five patients. *AJNR Am J Neuroradiol*. 1990; 11:887–892. [PubMed: 2120991]
- Harata N, Iwasaki Y. The blood-brain barrier and selective vulnerability in experimental thiamine-deficiency encephalopathy in the mouse. *Metab Brain Dis*. 1996; 11:55–69. [PubMed: 8815390]
- Hood L. Auditory neuropathy/Dys-synchrony disorder. *Otolaryngol Clin North Am*. 2015 in press.
- Huang LC, Barclay M, Lee K, Sasa P, Housley GD, Thorne PR, Montgomery JM. Synaptic profiles during neurite extension, refinement and retraction in the developing cochlea. *Neural Development*. 2012; 7:38. [PubMed: 23217150]
- Khimich D, Nouvian R, Pujol R, Tom Dieck S, Egner A, Gundelfinger ED, Moser T. Hair cell synaptic ribbons are essential for synchronous auditory signalling. *Nature*. 2005; 434:889–894. [PubMed: 15829963]
- Kiril JJ. Neuropathology of thiamine deficiency disorders. *Metab Brain Dis*. 1996; 11:9–17. [PubMed: 8815394]
- Kujawa SG, Liberman MC. Adding insult to injury: cochlear nerve degeneration after “temporary” noise-induced hearing loss. *J Neurosci*. 2009; 29:14077–14085. [PubMed: 19906956]
- Kujawa SG, Liberman MC. Synaptopathy in the noise-exposed and aging cochlea: primary neural degeneration in acquired sensorineural hearing loss. *Hear Res*. 2015 in press.
- Langlais PJ, Zhang SX, Savage LM. Neuropathology of thiamine deficiency: an update on the comparative analysis of human disorders and experimental models. *Metab Brain Dis*. 1996; 11:19–37. [PubMed: 8815388]
- Liberman MC, Tartaglino E, Fleming JC, Neufeld EJ. Deletion of SLC19A2, the high affinity thiamine transporter, causes selective inner hair cell loss and an auditory neuropathy phenotype. *J Assoc Res Otolaryngol*. 2006; 7:211–217. [PubMed: 16642288]
- Liberman LD, Wang H, Liberman MC. Opposing gradients of ribbon size and AMPA receptor expression underlie sensitivity differences among cochlear-nerve/hair-cell synapses. *J Neurosci*. 2011; 31:801–808. [PubMed: 21248103]
- Liberman MC, Liberman LD, Maison SF. Efferent feedback slows cochlear aging. *J Neurosci*. 2014; 34:4599–4607. [PubMed: 24672005]
- Liberman MC, Liberman LD, Maison SF. Chronic conductive hearing loss leads to cochlear degeneration. *PLoS ONE*. 2015; 10(11):e0142341. [PubMed: 26580411]
- Maison SF, Adams JC, Liberman MC. Olivocochlear innervation in the mouse: immunocytochemical maps, crossed versus uncrossed contributions, and transmitter colocalization. *J Comp Neurol*. 2003; 455:406–416. [PubMed: 12483691]
- Maison SF, Usubuchi H, Liberman MC. Efferent feedback minimizes cochlear neuropathy from moderate noise exposure. *J Neurosci*. 2013; 33:5542–5552. [PubMed: 23536069]

- Matsubara A, Laake JH, Davanger S, Usami S, Ottersen OP. Organization of AMPA receptor subunits at a glutamate synapse: a quantitative immunogold analysis of hair cell synapses in the rat organ of Corti. *J Neurosci*. 1996; 16:4457–4467. [PubMed: 8699256]
- Pangrsic T, Lasarow L, Reuter K, Takago H, Schwander M, Riedel D, Frank T, Tarantino LM, Bailey JS, Strenke N, Brose N, Müller U, Reisinger E, Moser T. Hearing requires otoferlin-dependent efficient replenishment of synaptic vesicles in hair cells. *Nat Neurosci*. 2010; 13:869–876. [PubMed: 20562868]
- Santarelli R, Del Castillo I, Rodríguez-Ballesteros M, Scimemi P, Cama E, Arslan E, Starr A. Abnormal cochlear potentials from deaf patients with mutations in the otoferlin gene. *J Assoc Res Otolaryngol*. 2009; 10:545–556. [PubMed: 19636622]
- Schmitz F, Konigstorfer A, Sudhof TC. RIBEYE, a component of synaptic ribbons: a protein's journey through evolution provides insight into synaptic ribbon function. *Neuron*. 2000; 28:857–872. [PubMed: 11163272]
- Schuknecht, HF. *Pathology of the Ear*. 2nd. Baltimore: Lea & Febiger; 1993. p. 1-503.1993
- Sergeyenko Y, Lall K, Liberman MC, Kujawa SG. Age-related cochlear synaptopathy: an early-onset contributor to auditory functional decline. *J Neurosci*. 2013; 33:13686–13694. [PubMed: 23966690]
- Starr A, Rance G. Auditory Neuropathy. *Handb Clin Neurol*. 2015; 129:495–508. [PubMed: 25726287]
- Taberner AM, Liberman MC. Response properties of single auditory nerve fibers in the mouse. *J Neurophysiol*. 2005; 93:557–569. [PubMed: 15456804]
- Victor, M.; Adams, RD.; Collins, GH. *The Wernicke-Korsakoff syndrome and related neurologic disorders due to alcoholism and malnutrition*. FA Davis; Philadelphia: 1989. p. 61-112.
- Wan G, Corfas G. No longer falling on deaf ears: Mechanisms of degeneration and regeneration of cochlear ribbon synapses. *Hear Res*. 2015; 329:1–10. [PubMed: 25937135]
- Wang Q, Green SH. Functional role of neurotrophin-3 in synapse regeneration by spiral ganglion neurons on inner hair cells after excitotoxic trauma in vitro. *J Neurosci*. 2011; 31:7938–7949. [PubMed: 21613508]
- Wang Y, Hirose K, Liberman MC. Dynamics of noise-induced cellular injury and repair in the mouse cochlea. *J Assoc Res Otolaryngol*. 2002; 3:248–268. [PubMed: 12382101]
- Xoinis K, Weirather Y, Mavoori H, Shaha SH, Iwamoto LM. Extremely low birth weight infants are at high risk for auditory neuropathy. *J Perinatol*. 2007; 27:718–723. [PubMed: 17703185]
- Yin Y, Liberman LD, Maison SF, Liberman MC. Olivocochlear innervation maintains the normal modiolar-pillar and habenular-cuticular gradients in cochlear synaptic morphology. *J Assoc Res Otolaryngol*. 2014; 15:571–583. [PubMed: 24825663]
- Zhang SX, Weilersbacher GS, Langlais PJ. Progression and reversibility of brainstem lesions produced by acute thiamine deficiency in rats. *Soc Neurosci Abstr*. 1994; 20:415.
- Zhang SX, Weilersbacher GS, Henderson SW, Corso T, Olney JW, Langlais PJ. Excitotoxic cytopathology, progression, and reversibility of thiamine deficiency-induced diencephalic lesions. *J Neuropathol Exp Neurol*. 1995; 54:255–267. [PubMed: 7876893]
- Zhong C, Jin L, Fei G. MR imaging of nonalcoholic Wernicke encephalopathy: a follow-up study. *AJNR Am J Neuroradiol*. 2005; 26:2301–2305. [PubMed: 16219836]

Highlights

Thiamine deprivation was induced during fetal development or early postnatal life.

Thiamine-deprivation resulted in significant anomalies in cochlear afferent or efferent innervation.

Auditory neuropathy from thiamine deprivation results from loss of inner hair cell synapses in mice.

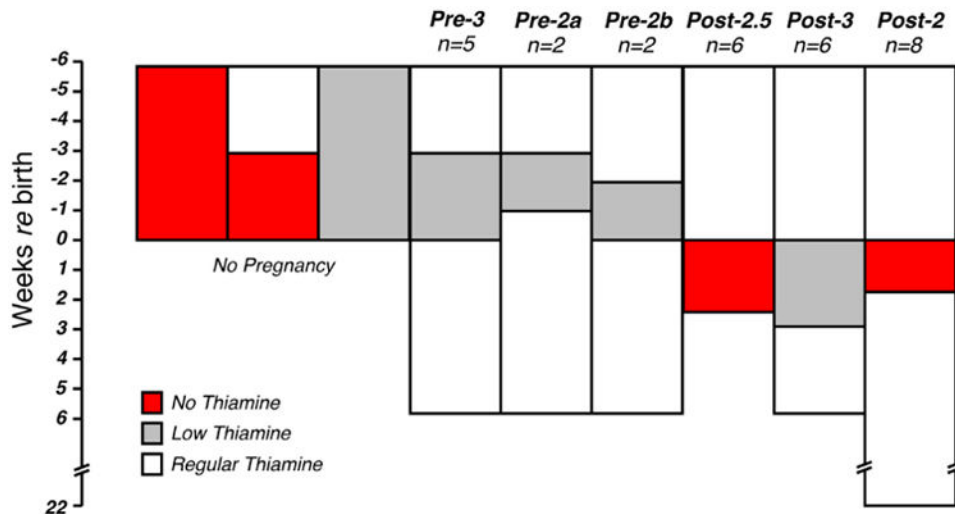


Figure 1. Schematic of the thiamine diet protocols. Mice were assigned to one of three groups: 1) Control animals, fed with regular chow (22 mg/kg thiamine); 2) Low-thiamine animals, fed with 0.2 mg/kg thiamine and 3) No-thiamine animals, fed with thiamine-free chow. Thiamine restriction was either applied prenatally (*Pre*) or postnatally (*Post*) for durations ranging from 2 to 6 wks. Females on a thiamine-free diet for 3 wks failed to become pregnant. On a low-thiamine diet, pregnancies went to full term if diet durations were 3 wks. Pups fed by mothers on a thiamine-free diet survived only if thiamine restriction was 18 days. Group sizes (n's) are indicated as number of ears evaluated.

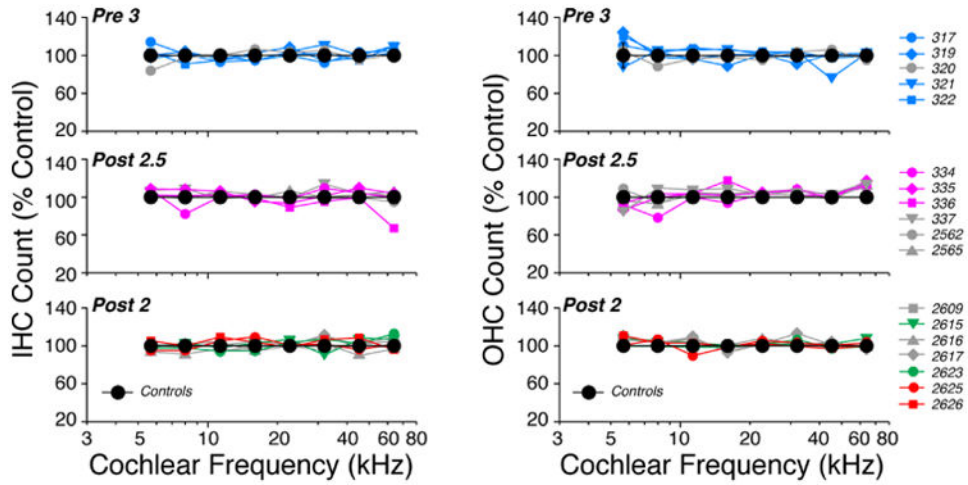


Figure 2. Neither pre- nor postnatal thiamine restriction led to any significant hair cell loss in any of the experimental groups. IHC and OHC counts are shown here from each ear from three groups as indicated: see Fig. 1 for diet details. Data are normalized to the mean counts per z-stack (spanning 78 microns of cochlear length) from Control ears. Control data are shown as means (\pm SEMs). In each panel, the ears represented by colored symbols are those displaying significant dysmorphology of afferent and/or efferent innervation: see Figs. 5, 6, 7, and 9, where the correspondence between symbols and case numbers is maintained.

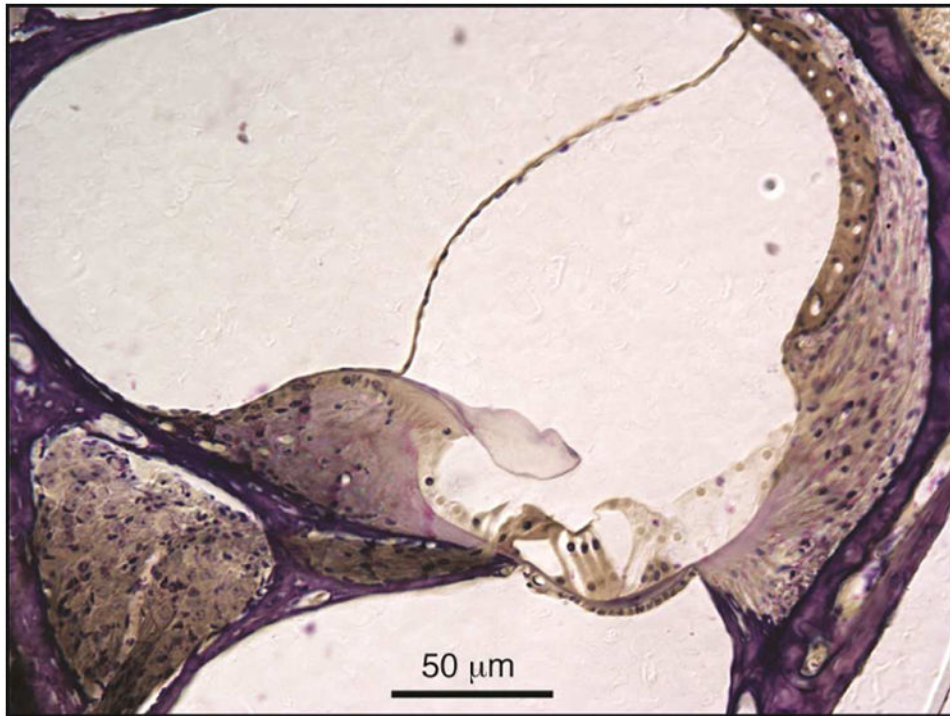


Figure 3.

In Post-2.5 mice, there were no obvious abnormalities in cochlear structures outside the sensory epithelium, as seen in this light micrograph of a plastic sections through the upper basal turn from right ear of case 334: data from the left ear of this case are described in Figure 5.

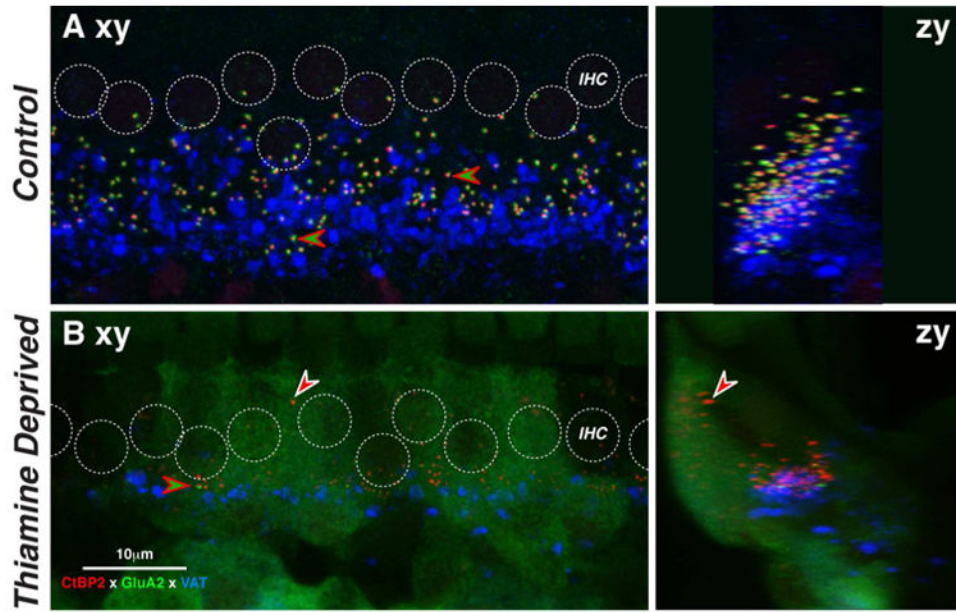


Figure 4. Mice with 18 days postnatal thiamine deprivation (*Post-2.5*) show dramatic loss of IHC synapses. Images are maximum projections of z-stacks through 10-11 adjacent IHCs from the 32-kHz region in a thiamine-deprived ear at P18 (**B**) and an age-matched control (**A**). Projections are viewed either in the xy (acquisition) plane (**left**) or the zy (digitally rotated) plane (**right**). Positions of IHC nuclei are indicated by dashed circles. Examples of paired pre- and post-synaptic puncta are indicated by red-green arrowhead. The location of one orphan ribbon is shown at the white-red arrowhead. Scale bar in **B** applies to all images. See text for further description.

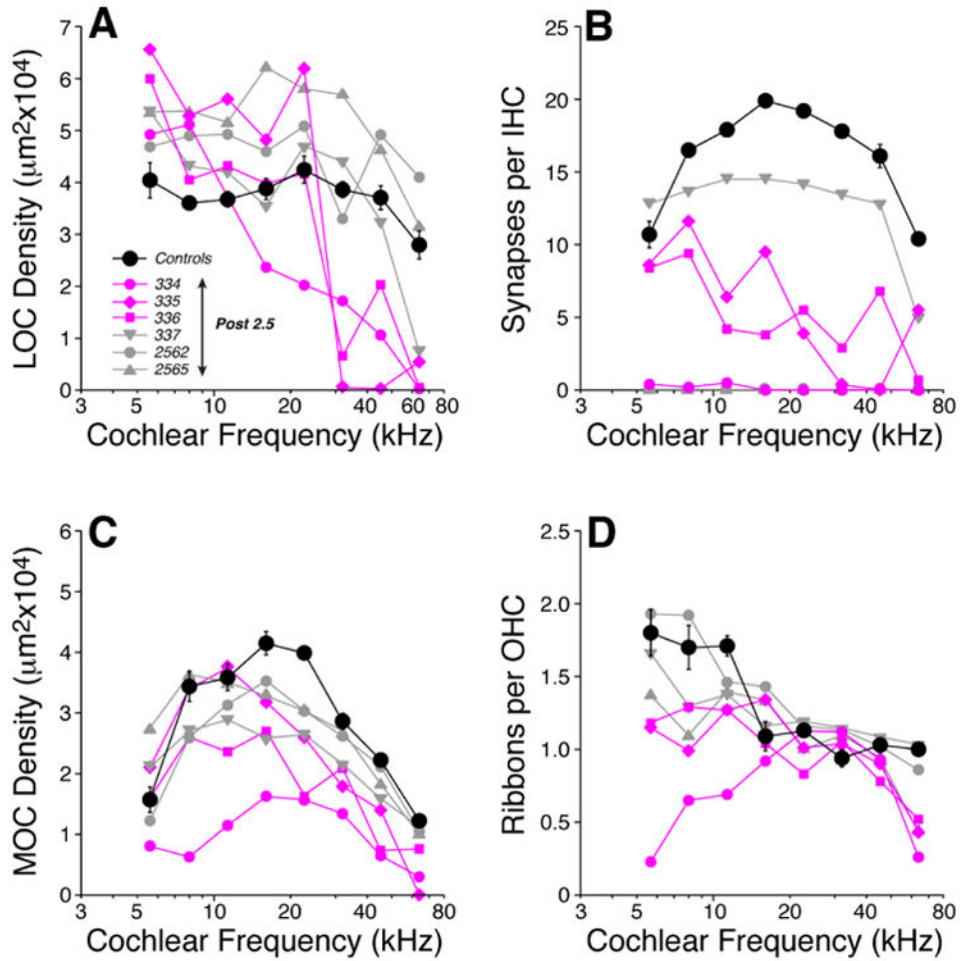


Figure 5. Mice with 18 days wks of postnatal thiamine deprivation (*Post-2.5*) are extremely weak and show profound changes in afferent and efferent innervation across all cochlear regions. LOC (A) and MOC (C) innervation densities, IHC synaptic counts (B) and OHC ribbon counts (D) in *Post-2.5* ears are compared to age-matched (P18) *Control* mean values (\pm SEMs). Key in A applies to all panels: three of the thiamine-deprived ears with the most dramatic reduction in IHC synaptic counts are shown in color. IHC synaptic counts from two *Post-2.5* mice (2562 and 2565) are missing from panel B because the background staining in the GluA2 channel was so high the signal from post-synaptic receptor patches was not interpretable.

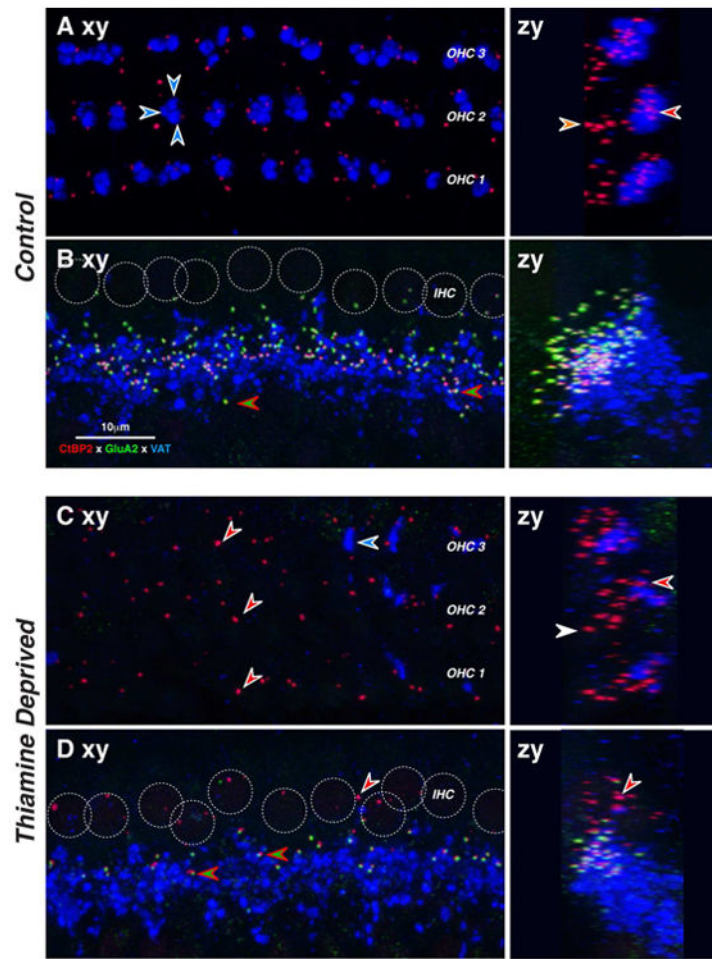


Figure 6.

Two weeks of postnatal thiamine deprivation (*Post-2*) can cause loss of IHC afferent synapses and MOC efferent terminals. Each image is the maximal projection of a confocal z-stack through the IHC (**B,D**) or OHC (**A,C**) areas, viewed either in the xy (acquisition) plane (**left**) or the zy (digitally rotated) plane (**right**). In normal IHCs, afferent synapses appear as pairs of red (anti-CtBP2) and green (anti-GluA2) puncta (**B,D**, *red-green arrowheads*). Positions of IHC nuclei are shown as dotted white circles (**B,D**). In normal OHCs, presynaptic ribbons are present, but no GluA2 puncta are visible. In thiamine-deprived IHCs, many GluA2 puncta are missing leaving orphan ribbons (**D**, *white-red arrowhead*). In thiamine deprived OHCs, the density of ribbons is reduced. OC efferent terminals appear in the blue (anti-VAT) channel. In control OHCs, 2-5 OC terminals contact the base of each OHC (**A**, white-blue arrowheads). In thiamine-deprived OHCs (**C**), density of OC terminals is greatly decreased (**C**). Scale in **B** applies to all micrographs, which are from the 11 kHz region of 22-wk old cochleas. See text for further description.

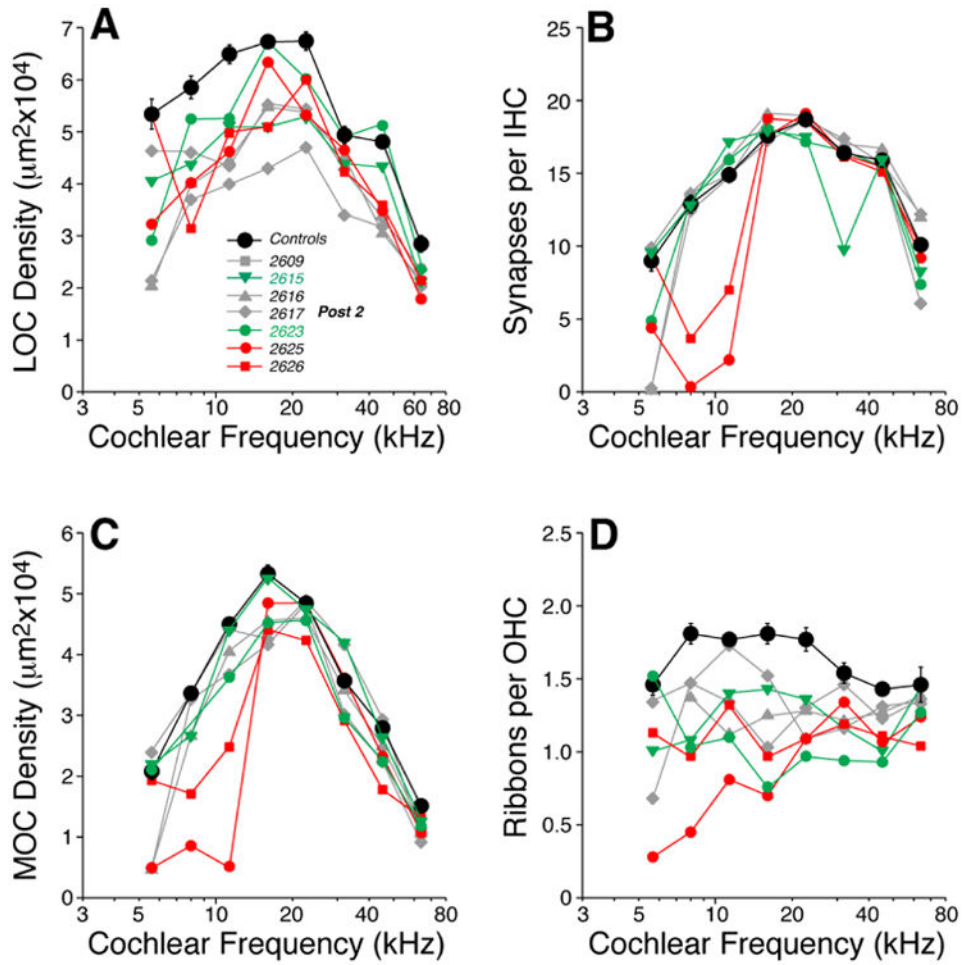


Figure 7. Two weeks of postnatal thiamine deprivation (*Post-2*) can lead to loss of afferent and efferent innervation, especially in the apical half of the cochlea. Panels **A-D** show the cochlear innervation abnormalities as seen at 22 wks. LOC (**A**) and MOC (**C**) innervation densities, IHC synaptic counts (**B**) and OHC ribbon counts (**D**) in individual *Post-2* ears are compared to mean values from age-matched *Control* (\pm SEMs). Key in **A** applies to all panels: red symbols indicate cases with dramatic reduction of IHC synapses in the apex (**B**); green symbols indicate cases with exceptionally weak DPOAEs at high frequencies (Fig. 8).

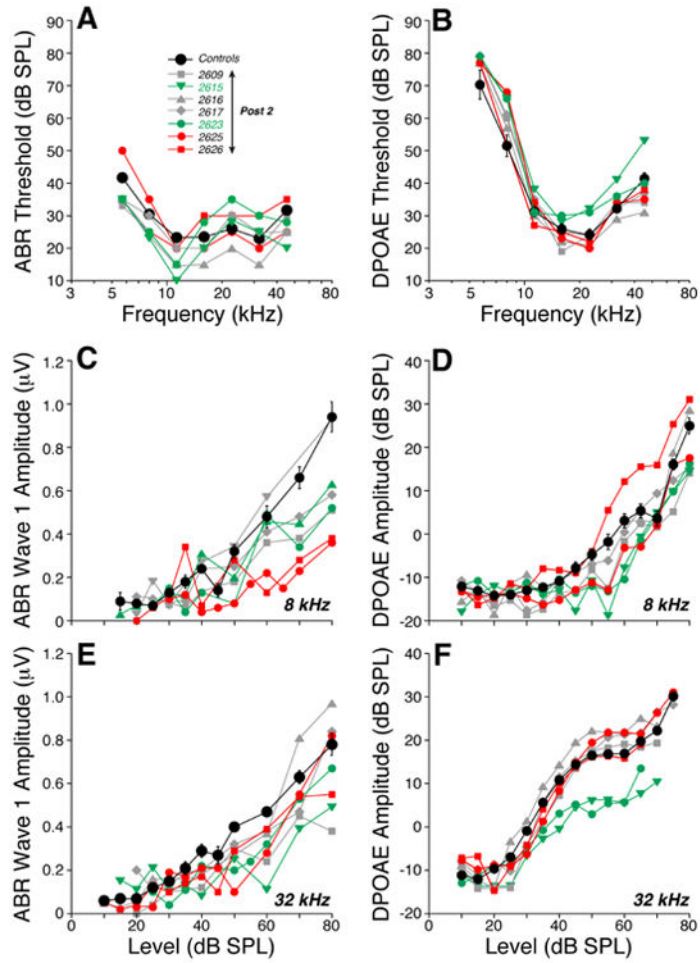


Figure 8. The apical loss of IHC synapses in the *Post-2* ears (Fig. 7B) produces the expected anomalies in cochlear function: i.e. low suprathreshold amplitudes for ABR Wave 1 at 8 kHz (C) without large threshold changes in ABRs (A) or DPOAEs (B). Absolute thresholds (A,B) and suprathreshold amplitudes are shown at 8 kHz (C-D) and 32 kHz (E-F) for DPOAEs (B,D,F) and for wave 1 of the ABR (A,C,E) in *Post-2* mice compared to mean values for age-matched Controls (\pm SEMs). All measurements were done at 22 wks. Key in A applies to all panels: red symbols are for cases with dramatic reduction of IHC synapses in the apex (Fig. 7); green symbols are for cases with exceptionally weak DPOAEs at high frequencies (B,F).

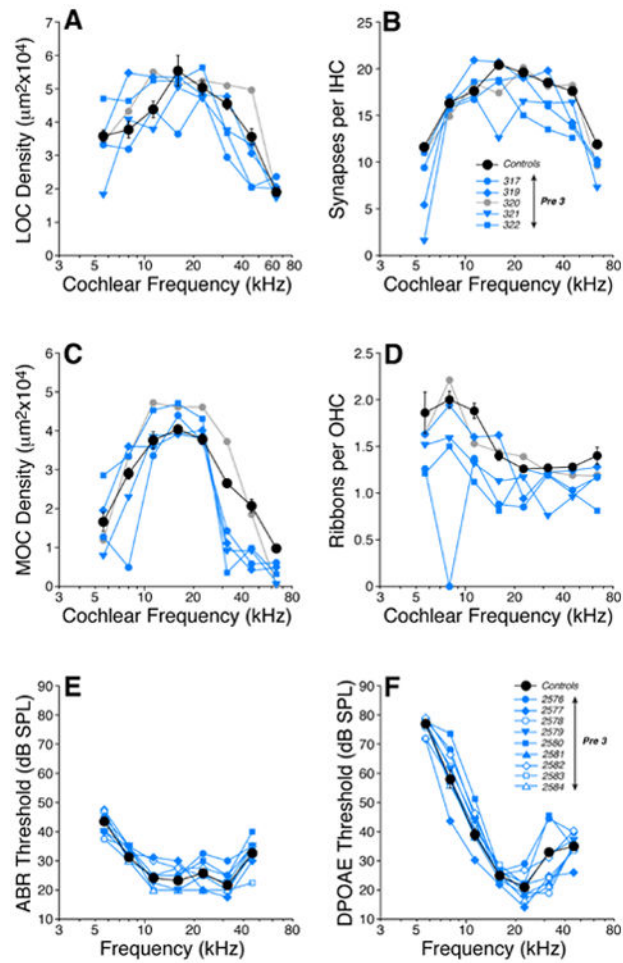


Figure 9.

Prenatal thiamine restriction for 3 wks (*Pre-3*) leads to a moderate loss of afferent and efferent innervation without significant changes in cochlear thresholds. Panels **A-D** show the cochlear innervation abnormalities found in the offspring of mice fed on a low-thiamine chow during the last 3 wks of pregnancy (*Pre-3* in Fig. 1). LOC (**A**) and MOC (**C**) innervation densities, inner hair cell synaptic counts (**B**) and outer hair cell ribbon counts (**D**) in each of the five *Pre-3* mice are compared to mean values from age-matched *Controls* (\pm SEMs). Key in **B** applies to panels **A-D**: blue symbols are four cases with exceptionally low MOC densities in the cochlear base (**C**). Panels **E-F** show thresholds for ABRs (**E**) and DPOAEs (**F**) in *Pre-3* mice compared to mean values for age-matched *Controls* (\pm SEMs). All measurements were done at 6 wks. Key in **E** also applies to **F**.

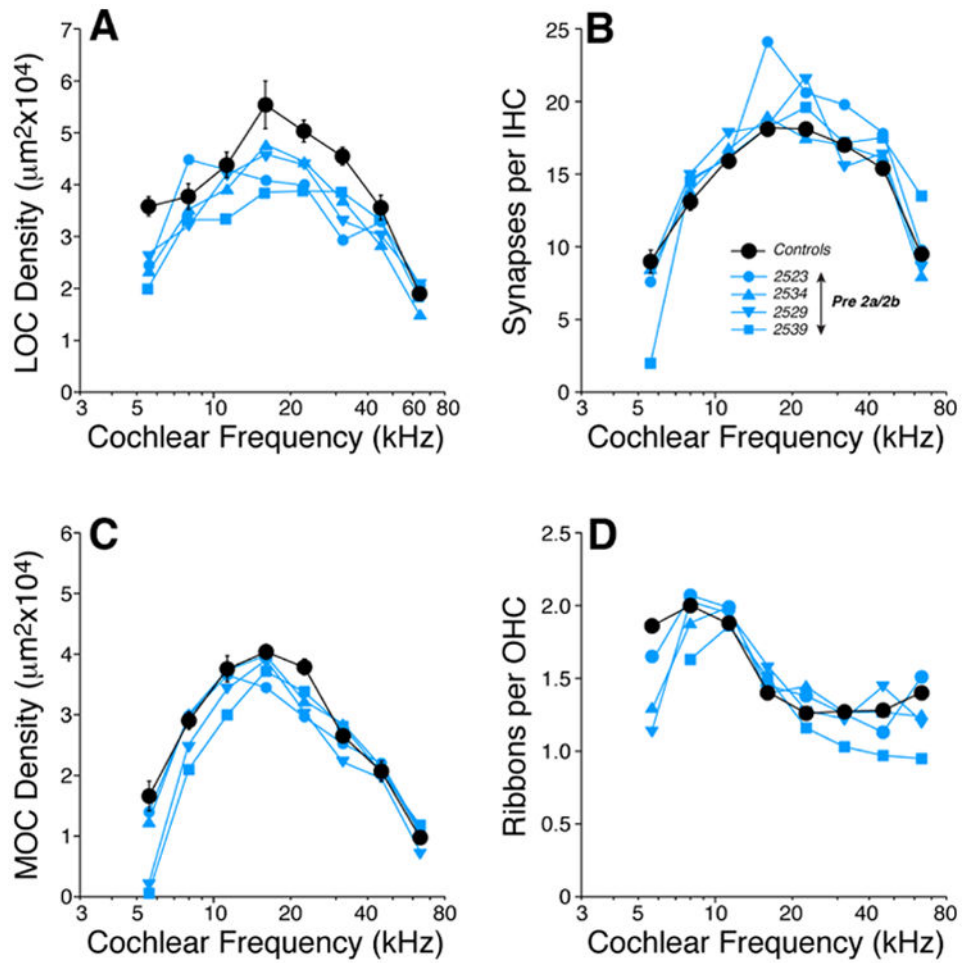


Figure 10.

Prenatal thiamine restriction for 2 wks (*Pre-2*) leads to a moderate loss of efferent innervation in both the OHC and IHC areas. Panels **A-D** show the cochlear innervation abnormalities found in the offspring of mice fed on a low-thiamine chow during the last 2 wks of pregnancy (*Pre-2a* and *2b* in Figure 1). LOC (**A**) and MOC (**C**) innervation densities, inner hair cell synaptic counts (**B**) and outer hair cell ribbon counts (**D**) in each of the 4 *Pre-2* mice are compared to mean values from age-matched *Controls* (\pm SEMs). Key in **B** applies to all panels.